JCB Article

Bro1 coordinates deubiquitination in the multivesicular body pathway by recruiting Doa4 to endosomes

Natalie Luhtala and Greg Odorizzi

Molecular, Cellular, and Developmental Biology, University of Colorado, Boulder, CO 80309

Ubiquitination directs the sorting of cell surface receptors and other integral membrane proteins into the multivesicular body (MVB) pathway. Cargo proteins are subsequently deubiquitinated before their enclosure within MVB vesicles. In *Saccharomyces cerevisiae,* Bro1 functions at a late step of MVB sorting and is required for cargo protein deubiquitination. We show that the loss of Bro1 function is suppressed by the overexpression of *DOA4,* which encodes the ubiquitin thiolesterase required for the removal of ubiquitin from MVB cargoes. Overexpression of *DOA4* restores cargo protein deubiquitination and sorting via the MVB pathway and reverses the abnormal endosomal morphology typical of *bro1* mutant cells, resulting in the restoration of multivesicular endosomes. We further demonstrate that Doa4 interacts with Bro1 on endosomal membranes and that the recruitment of Doa4 to endosomes requires Bro1. Thus, our results point to a key role for Bro1 in coordinating the timing and location of deubiquitination by Doa4 in the MVB pathway.

Introduction

Multivesicular bodies (MVBs) are late endosomes containing lumenal vesicles formed by invagination of the limiting endosomal membrane. The MVB vesicles are delivered into the hydrolytic lumen of the lysosome/vacuole upon fusion of the limiting MVB membrane with the lysosomal/vacuolar membrane. A variety of cell surface receptors down-regulated from the plasma membrane are sorted into MVB vesicles en route to being degraded, including many growth factor receptor tyrosine kinases in animals and G protein-coupled pheromone receptors in the budding yeast *Saccharomyces cerevisiae*. In yeast, several biosynthetic enzymes are also sorted into MVB vesicles during their transport from the Golgi to the vacuole (for review see Hicke and Dunn, 2003).

Ubiquitination mediates the sorting of integral membrane proteins into the MVB pathway. Ubiquitin (Ub) is a highly conserved 76-aa polypeptide that is covalently linked to specific protein substrates by a cascade of Ub-conjugation enzymes. Ubiquitination was first characterized to occur on soluble proteins that are polyubiquitinated via the attachment of a chain of four or more Ub subunits, which targets these substrates for degradation by the proteasome (Weissman, 2001). In contrast, MVB cargo proteins are monoubiquitinated via the linkage of a single Ub subunit (or a chain of two to three subunits) to their cytoplasmic domains (Hicke and Dunn, 2003). Ub is removed from both polyubiquitinated and monoubiquitinated proteins by deubiquitinating enzymes, thereby enabling cells to maintain a constant pool of Ub (Weissman, 2001; Wing, 2003).

The sorting of ubiquitinated MVB cargoes is controlled by class E Vps proteins, a set of conserved cytoplasmic proteins that associate with endosomal membranes. Several class E Vps proteins coassemble into distinct complexes that bind to ubiquitinated cargo proteins and guide them into the MVB pathway. In yeast, cargoes initially bind the Vps27–Hse1 complex and subsequently interact with the ESCRT-I complex (Vps23, Vps28, and Vps37; Bilodeau et al., 2003; Katzmann et al., 2003). The ESCRT-II (Vps22, Vps25, and Vps36) and ESCRT-III (Vps2, Vps20, Vps24, and Snf7) complexes function downstream of ESCRT-I (Babst et al., 2002a, b), but their precise roles are not known. In mammalian cells, class E Vps orthologues also mediate the sorting of MVB cargo proteins (Hicke and Dunn, 2003). Furthermore, this machinery is exploited by certain enveloped viruses in order to escape from host cells. For example, Tsg101, the mammalian orthologue of yeast Vps23, is recruited to HIV-1 budding sites at the plasma membrane by directly interacting

The online version of this article contains supplemental material.

Address correspondence to Greg Odorizzi, Molecular, Cellular, and Developmental Biology, 347 UCB, University of Colorado, Boulder, CO 80309-0347. Tel.: (303) 735-0179. Fax: (303) 492-7744. email: odorizzi@colorado.edu

Key words: endosomes; protein sorting; ubiquitin thiolesterase

Abbreviations used in this paper: CPS, carboxypeptidase S; CPY, carboxypeptidase Y; CPY-Inv, CPY-invertase; DIC, differential interference contrast; MVB, multivesicular body; Ub, ubiquitin; UBP, ubiquitin-specific processing protease.

with ubiquitinated viral Gag proteins (for review see Pornillos et al., 2002).

Additional class E Vps proteins function in the MVB pathway in yeast, including Vps4, an AAA-type ATPase that catalyzes the dissociation of ESCRT complexes from endosomal membranes (Babst et al., 2002a,b). Vps4 also functions in the endosomal dissociation of Bro1, a class E Vps protein required for the deubiquitination of cargo proteins at a late stage of the MVB pathway downstream of the ESCRT-III complex (Nikko et al., 2003; Odorizzi et al., 2003). The association of Bro1 with endosomes requires Snf7 (Odorizzi et al., 2003), and the mammalian Bro1 orthologue, Alix (also known as Aip1), has been shown to bind the mammalian Snf7 orthologue, CHMP4b (Katoh et al., 2003; Martin-Serrano et al., 2003; Peck et al., 2004; Strack et al., 2003; von Schwedler et al., 2003). Studies of HIV-1–infected cells have revealed that Alix/Aip1 also binds Tsg101 during viral budding from the plasma membrane (Strack et al., 2003; von Schwedler et al., 2003), suggesting that Alix/Aip1 bridges an interaction between the ESCRT-I and -III complexes. Interestingly, Alix/Aip1 binds specifically to synthetic liposomes containing lysobisphosphatidic acid and appears to antagonize the ability of this unconventional phospholipid to promote membrane invagination (Matsuo et al., 2004), but the role of Alix/Aip1 in controlling membrane dynamics is not clear.

Here, we report that the defects in MVB sorting caused by the loss of Bro1 function in yeast are suppressed by overexpression of the *DOA4* gene, which encodes the Ub thiolesterase required for the removal of Ub from MVB cargo proteins (Dupre and Haguenauer-Tsapis, 2001; Katzmann et al., 2001; Losko et al., 2001). Specifically, our data demonstrate that high-copy expression of *DOA4* restores cargo protein deubiquitination and subsequent transport via the MVB pathway in *bro1* mutant cells. The catalytic activity of Doa4 is essential for its role as a suppressor, indicating that the mechanism of suppression involves substrate deubiquitination. Furthermore, the multivesicular morphology of late endosomes, which is abnormal in *bro1* mutant cells, is restored by the overexpression of *DOA4*. The ability of high-copy *DOA4* to suppress the loss of Bro1 function is explained by our finding that Bro1 is essential for the localization of Doa4 to endosomes and that Bro1 and Doa4 physically interact on endosomal membranes. Therefore, Bro1 has a crucial role in coordinating substrate deubiquitination in the MVB pathway by recruiting Doa4 to endosomes.

Results

The coiled-coil domain of Bro1 is essential for MVB sorting

Many class E Vps proteins have one or more coiled-coil domains, which are structural elements that typically mediate protein–protein interactions. Bro1 has a central coiled-coil domain spanning residues 543-583 (Fig. 1 A). We constructed a mutant allele (*bro1*$^{\Delta CC}$) in which the sequence encoding this domain had been deleted, and then integrated the *bro1*$^{\Delta CC}$ allele by homologous recombination into the genome in place of the wild-type *BRO1* gene. To determine whether MVB sorting was functional in *bro1*$^{\Delta CC}$ cells, we examined the intracellular localization of a fusion protein in which GFP was attached to the cytoplasmic domain of carboxypeptidase S (CPS), a biosynthetic enzyme that is sorted via the MVB pathway during its transport from the Golgi to the vacuole (Odorizzi et al., 1998). GFP-CPS was found entirely within the vacuole lumen of wild-type cells (Fig. 1 B). In contrast, GFP-CPS in *bro1*$^{\Delta CC}$ cells was observed at the vacuole membrane (Fig. 1 B), which is indicative of a defect in sorting of the fusion protein via the MVB pathway (Odorizzi et al., 1998). GFP-CPS was also mislocalized to class E compartments (Fig. 1 B, arrowheads), abnormal late endosomal structures that occur in all class E *vps* mutant cells. A similar defect in the localization of GFP-CPS was seen in *bro1*Δ cells in which the entire *BRO1* coding sequence had been deleted (Fig. 1 B). In addition, we observed in both *bro1*$^{\Delta CC}$ and *bro1*Δ mutant cells that Ste3-GFP, an MVB cargo protein endocytosed from the plasma membrane (Urbanowski and Piper, 2001), failed to be sorted into the vacuole lumen (unpublished data). Thus, the coiled-coil domain of Bro1 is essential for the function of Bro1 in the MVB pathway.

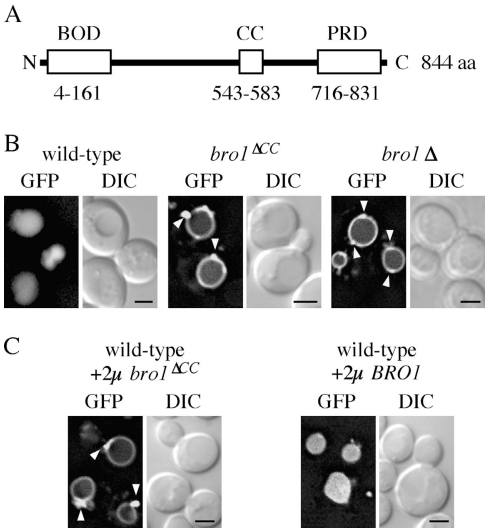

Figure 1. **The coiled-coil domain of Bro1 is essential for CPS transport via the MVB pathway.** (A) Schematic diagram of Bro1 indicating the locations of the Bro1 domain (BOD), the coiled-coil domain (CC), and the proline-rich domain (PRD). (B and C) Fluorescence and DIC microscopy of BHY10, GOY57 and KGY1 cells expressing a *GFP-CPS* fusion. In C, cells were transformed with a high-copy (2 μ) plasmid encoding *bro1*$^{\Delta CC}$ or wild-type *BRO1*. Arrowheads indicate class E compartments (B) and class E compartment-like structures (C). Bars, 2.5 μm.

Interestingly, when we overexpressed the *bro1*$^{\Delta CC}$ mutant allele in wild-type cells, GFP-CPS was mislocalized both to the vacuole membrane and to a structure that resembles the class E compartment (Fig. 1 C). In contrast, overexpression of the wild-type *BRO1* gene had no deleterious effect on the localization of GFP-CPS (Fig. 1 C). The overexpression of *bro1*$^{\Delta CC}$, therefore, causes a dominant-negative phenotype, possibly because the mutant gene product interferes with the function of the wild-type Bro1 protein.

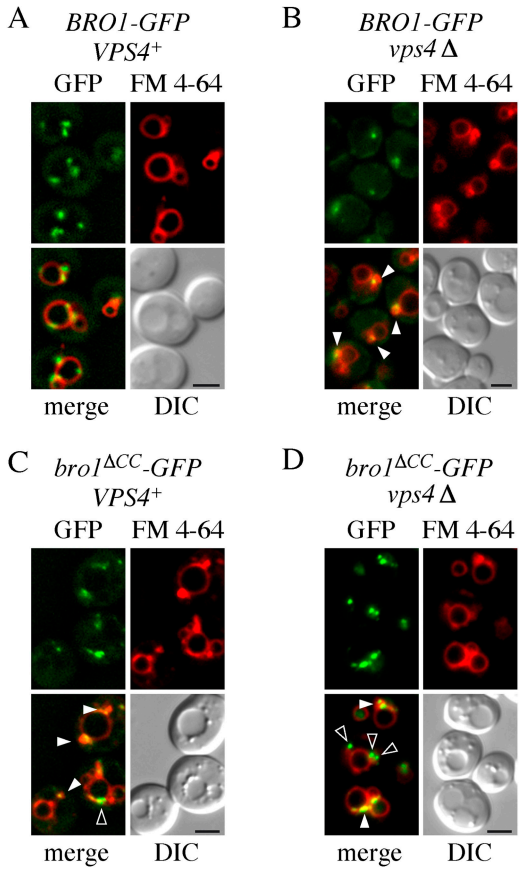

Figure 2. **The Bro1 coiled-coil domain is not required for endosomal localization of Bro1.** Fluorescence and DIC microscopy of DMY1 (A), DMY2 (B), DBY15 (C), and DBY18 (D) cells stained with FM 4-64. Closed arrowheads indicate class E compartments costained by FM 4-64. Open arrowheads indicate GFP-positive structures not labeled by FM 4-64. Bars, 2.5 μm.

The coiled-coil domain is not required for Bro1 to associate with endosomes

We previously demonstrated that Bro1 is a cytoplasmic protein which associates with endosomal compartments and that the dissociation of Bro1 from endosomes requires the ATPase activity of Vps4 (Odorizzi et al., 2003). Thus, when we replaced the wild-type *BRO1* gene with a genomically integrated *BRO1-GFP* gene fusion in cells that have normal Vps4 function (*VPS4*$^+$), we observed multiple fluorescent punctate structures in addition to diffuse cytoplasmic fluorescence (Fig. 2 A). Upon deletion of the *VPS4* gene (*vps4*Δ), the GFP fluorescence was concentrated at class E compartments, which had formed in these cells due to the absence of Vps4 activity (Fig. 2 B). The cells in these experiments shown in Fig. 2 (and in Figs. 6, 7, and 9) were also labeled by a brief pulse of FM 4-64 followed by incubation in label-free medium. FM 4-64 is a fluorescent lipophilic compound that intercalates into the plasma membrane and is endocytosed, resulting in the staining of vacuole membranes and class E compartments (Vida and Emr, 1995).

To determine if the coiled-coil domain is required for the association of Bro1 with endosomes, we integrated a *bro1*$^{\Delta CC}$-GFP gene fusion in place of the wild-type *BRO1* gene. Both in *VPS4*$^+$ and *vps4*Δ cells expressing *bro1*$^{\Delta CC}$-GFP, fluorescence was localized at class E compartments that were costained by FM 4-64 (Fig. 2, C and D, closed arrowheads). Class E compartments had formed in *VPS4*$^+$ cells expressing *bro1*$^{\Delta CC}$-GFP in place of wild-type *BRO1* due to the fact that the coiled-coil domain is required for the function of Bro1 in the MVB pathway (Fig. 1). Electron microscopic analysis of immunogold labeled cell sections confirmed that the bro1$^{\Delta CC}$-GFP fusion protein was, indeed, associated with class E compartments in both *VPS4*$^+$ and *vps4*Δ cells (not depicted). Interestingly, in contrast with wild-type Bro1-GFP, bro1$^{\Delta CC}$-GFP was also localized in both strains to additional punctate structures that were not labeled by FM 4-64 (Fig. 2, C and D, open arrowheads). However, the localization of bro1$^{\Delta CC}$-GFP to class E compartments indicates that the coiled-coil domain per se is not required for the localization of Bro1 to late endosomes.

Overexpression of *DOA4* suppresses CPY sorting defects in *bro1* mutant cells

To identify proteins that may be able to restore normal function of the MVB pathway when over-produced in the *bro1*$^{\Delta CC}$ mutant strain, we designed a genetic screen based upon another phenotype observed in *bro1* mutant cells. In addition to MVB sorting defects, *bro1* mutants inefficiently sort a soluble vacuolar enzyme, carboxypeptidase Y (CPY). Newly synthesized CPY is transported from the ER to the Golgi, where it binds a transmembrane receptor, Vps10. In wild-type cells (Fig. 3 A), the Vps10–CPY complex is sorted from the Golgi to endosomes, whereupon CPY dissociates from Vps10, and the receptor recycles back to the Golgi, whereas CPY is transported further toward the vacuole (Cereghino et al., 1995; Cooper and Stevens, 1996). The class E compartments that are formed in *bro1* mutant cells prevent Vps10 from efficiently recycling to the Golgi (Fig. 3 B), resulting in a significant portion of newly synthesized CPY entering by default into the secretory pathway (Odorizzi et al., 2003). Thus, the secretion of CPY by *bro1* mutant cells is likely to be an indirect consequence of the aberrant endosomal morphology that occurs upon the loss of Bro1 function.

The percentage of total cellular CPY that is secreted can be measured quantitatively using a colorimetric assay that monitors the enzymatic activity of a CPY-invertase (CPY-Inv) fusion protein (Darsow et al., 2000). As shown in Fig. 3 C, wild-type cells secreted ~1% of CPY-Inv, whereas *bro1*Δ cells secreted 10–15 times this amount. The *bro1*$^{\Delta CC}$ mutant strain secreted nearly the same percentage as *bro1*Δ cells (Fig. 3 C), which is consistent with the coiled-coil domain being essential for the function of Bro1 in the MVB pathway.

The colorimetric assay for invertase activity can also be used to detect the secretion of CPY-Inv by cells growing on solid medium (Darsow et al., 2000). We used this assay in a genetic screen to identify any gene that, when overexpressed in *bro1*$^{\Delta CC}$ cells, reduced the amount of secreted CPY-Inv. We reasoned that such a high-copy suppressor would encode a protein that interacts with Bro1 and would be able to restore normal function of the MVB pathway when over produced. Thus, we transformed the *bro1*$^{\Delta CC}$ strain with a high-copy plasmid library of yeast genomic DNA and identified colonies that secreted less CPY-Inv relative to the *bro1*$^{\Delta CC}$ strain. One clone contained a plasmid that could reproduc-

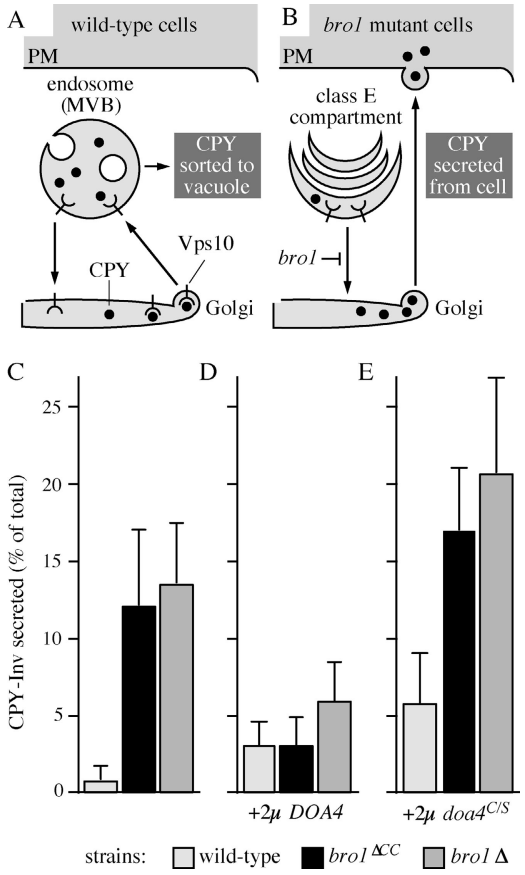

Figure 3. ***DOA4* overexpression in *bro1* mutant cells suppresses CPY-Inv secretion.** Schematic diagram of the trafficking of CPY in wild-type cells (A) and in *bro1* mutant cells (B). Not depicted in A is the fusion of the endosome/MVB with the vacuole. PM, plasma membrane. (C–E) Quantitation of CPY-Inv secretion by BHY10, GOY57, and KGY1 cells transformed either with the empty high-copy (2 μ) plasmid (C), the 2 μ plasmid containing the wild-type *DOA4* gene (D), or the 2 μ plasmid containing the mutant $doa4^{C/S}$ allele (E). The bar graph depicts the mean ± standard error from multiple independent experiments (Table I).

ibly suppress CPY-Inv secretion. Nucleotide sequence analysis revealed that this suppressor plasmid contained a 7.3-kb fragment of chromosome IV that includes the complete ORF of five genes, one of which is *DOA4*.

The *DOA4* gene product is a member of the Ub-specific processing protease (UBP) family of Ub thiolesterases (Wing, 2003). Doa4 is the UBP required for removal of Ub from the cytoplasmic domain of CPS and other MVB cargo proteins (Dupre and Haguenauer-Tsapis, 2001; Katzmann et al., 2001; Losko et al., 2001), and subcloning confirmed that *DOA4* is the gene within the library plasmid responsible for suppression of the $bro1^{\Delta CC}$ phenotype (unpublished data). The suppression of CPY-Inv secretion mediated by *DOA4* overexpression is shown in Fig. 3 D and Table I. High-copy *DOA4* reduced the percentage of CPY-Inv secreted by $bro1^{\Delta CC}$ cells by approximately threefold. In contrast, *DOA4* overexpression resulted in approximately threefold more CPY-Inv secreted by wild-type cells, indicating that high-copy *DOA4* caused a subtle dominant-negative phenotype. Surprisingly, *DOA4* overexpression reduced by approximately twofold the amount of CPY-Inv secreted by *bro1*Δ cells, indicating a partial bypass of Bro1.

The catalytic region of UBP enzymes have a conserved three-domain architecture that includes a critical cysteine residue, which forms a thiolester bond with Ub (Hu et al., 2002). We constructed a point mutant allele ($doa4^{C/S}$) in which the corresponding cysteine in Doa4 (Cys^{571}) had been changed to a serine residue. The $doa4^{C/S}$ allele failed to suppress CPY-Inv secretion when overexpressed in either $bro1^{\Delta CC}$ or *bro1*Δ cells. Instead, $doa4^{C/S}$ overexpression enhanced the mutant phenotype in both strains and caused a stronger dominant-negative phenotype in wild-type cells (Fig. 3 E). Catalytic activity, therefore, is essential for high-copy *DOA4* to suppress CPY-Inv secretion caused by the loss of Bro1 function.

Because high-copy *DOA4* partially suppressed the *bro1*Δ phenotype, we determined whether the loss of any class E Vps protein could be bypassed by *DOA4* overexpression. We transformed either the empty library vector or the library plasmid containing *DOA4* into strains in which individual class E *VPS* genes had been deleted, and then measured the percentage of secreted CPY-Inv (Table I). Suppression failed to occur in strains in which components of the ESCRT-I, -II, or -III complexes had been deleted (Table I). High-copy *DOA4* also could not suppress the loss of other class E Vps proteins, including Vps27 (Table I), which functions upstream of the ESCRT-I complex in the recognition of ubiquitinated MVB cargo proteins (Bilodeau et al., 2003; Katzmann et al., 2003). Interestingly, *DOA4* overexpression suppressed the secretion of CPY-Inv by *vps4*Δ cells but could not suppress either *bro1*Δ *vps4*Δ or $bro1^{\Delta CC}$ *vps4*Δ double mutant cells (Table I). These observations suggest that high-copy *DOA4* suppresses the CPY sorting defects in *bro1* and *vps4* mutants by different mechanisms.

High-copy *DOA4* suppresses CPS deubiquitination and sorting defects in $bro1^{\Delta CC}$ mutant cells

We had hypothesized that a high-copy suppressor of the aberrant secretion of CPY-Inv by *bro1* mutant cells would restore normal function of the MVB pathway. Indeed, when we examined the localization of GFP-CPS in $bro1^{\Delta CC}$ cells overexpressing *DOA4*, most of the fusion protein was seen inside the vacuole lumen, with only a small amount detected on the vacuole membrane (Fig. 4 A). Fluorescent punctate structures were not evident in these cells, suggesting that class E compartment formation was significantly reduced. We also observed more GFP-CPS within the vacuole lumen of *bro1*Δ cells overexpressing *DOA4* (Fig. 4 B) compared with *bro1*Δ cells alone (Fig. 1 B). However, compared with $bro1^{\Delta CC}$ cells that overexpress *DOA4* (Fig. 4 A), much more GFP-CPS in *bro1*Δ cells overexpressing *DOA4* was seen at the vacuole membrane and at structures that resembled class E compartments (Fig. 4 B). Thus, high-copy *DOA4* is much less efficient at suppressing the defect in GFP-CPS sorting in *bro1*Δ compared with $bro1^{\Delta CC}$ cells.

Although the overexpression of *DOA4* in *vps4*Δ cells suppressed CPY-Inv secretion (Table I), it did not restore the sorting of GFP-CPS into the vacuole lumen. As shown in Fig. 4 D, GFP-CPS was mislocalized to the vacuole mem-

Table I. **Effect of *DOA4* over-expression on CPY-Inv secretion and GFP-CPS sorting**

Strain	−/+ 2 μ *DOA4*[a]	Percentage of secreted CPY-Inv[b]	GFP-CPS localization
Wild-type	−	1.0 ± 2.1[c] (5)[d]	VL[e]
	+	2.8 ± 1.5 (4)	VL
bro1$^{\Delta CC}$	−	11.5 ± 4.7 (24)	VM + EC[f]
	+	3.7 ± 2.5 (7)	VL
*bro1*Δ	−	13.0 ± 3.8 (6)	VM + EC
	+	5.6 ± 2.4 (5)	VL + VM + EC
*vps4*Δ	−	39.4 ± 2.5 (3)	VM + EC
	+	5.2 ± 1.7 (3)	VM + EC
*bro1*Δ *vps4*Δ	−	43.7 ± 6.9 (3)	VM + EC
	+	46.0 ± 7.1 (3	VM + EC
bro1$^{\Delta CC}$ *vps4*Δ	−	35.2 ± 2.9 (3)	VM + EC
	+	35.9 ± 4.1 (3)	VM + EC
ESCRT-I mutants			
*vps23*Δ	−	20.0 ± 5.9 (3)	VM + EC
	+	17.6 ± 2.0 (3)	VM + EC
*vps28*Δ	−	13.4 ± 1.2 (3)	VM + EC
	+	21.7 ± 4.2 (3)	VM + EC
*vps37*Δ	−	16.3 ± 1.7 (3)	VL[g]
	+	15.8 ± 1.3 (3)	VL
ESCRT-II mutants			
*vps22*Δ	−	20.1 ± 4.5 (3)	VM + EC
	+	20.5 ± 6.1 (3)	VM + EC
*vps25*Δ	−	23.1 ± 1.0 (3)	VM + EC
	+	20.7 ± 0.9 (3)	VM + EC
*vps36*Δ	−	24.2 ± 6.3 (3)	VM + EC
	+	20.6 ± 4.1 (3)	VM + EC
ESCRT-III mutants			
*vps2*Δ	−	25.2 ± 5.0 (3)	VM + EC
	+	27.8 ± 6.5 (3)	VM + EC
*vps24*Δ	−	29.1 ± 4.3 (3)	VM + EC
	+	30.9 ± 4.4 (3)	VM + EC
*vps20*Δ	−	24.2 ± 2.9 (3)	VM + EC
	+	20.1 ± 6.5 (3)	VM + EC
*snf7*Δ	−	25.8 ± 5.0 (3)	VM + EC
	+	24.6 ± 1.1 (3)	VM + EC
Other class E *vps* mutants tested			
*vps27*Δ	−	28.0 ± 1.5 (3)	VM + EC
	+	26.5 ± 2.6 (3)	VM + EC
*nhx1*Δ	−	41.8 ± 13.0 (3)	VL[g]
	+	39.1 ± 13.0 (3)	VL
*vps60*Δ	−	17.7 ± 1.3 (3)	VM + EC
	+	19.0 ± 5.5 (3)	VM + EC

[a]Strains were transformed with the empty 2 μ vector (−) or the 2 μ vector containing *DOA4* (+).
[b]The percentage of total cellular CPY-Inv secreted by cells.
[c]Mean ± standard error.
[d]Number of independent experiments.
[e]Vacuole lumen.
[f]Vacuole membrane and class E compartment.
[g]There was no noticeable defect in GFP-CPS sorting in *vps37*Δ and *nhx1*Δ cells.

brane and the class E compartment in *vps4*Δ cells overexpressing *DOA4*, which is identical to the mislocalization of GFP-CPS in *vps4*Δ cells (Odorizzi et al., 1998). High-copy *DOA4* also failed to restore the sorting of GFP-CPS via the MVB pathway in other class E *vps* mutants (Table I).

In *doa4* mutant cells, CPS and other MVB cargoes accumulate in their ubiquitinated forms (Dupre and Haguenauer-Tsapis, 2001; Katzmann et al., 2001; Losko et al., 2001). We recently showed that ubiquitinated CPS (Ub-CPS) also accumulates in *bro1*Δ cells (Odorizzi et al., 2003). Therefore, we investigated whether *DOA4* overexpression could alleviate the defect in CPS deubiquitination that occurs upon loss of Bro1 function. Because the deubiquitination of CPS is normally efficient, Ub-CPS was difficult to detect in wild-type cells, but a significant amount of Ub-CPS was observed in *bro1*$^{\Delta CC}$ cells (Fig. 4 E). As shown in Fig. 4 (E and F), overexpression of *DOA4* completely restored CPS deubiquitination in *bro1*$^{\Delta CC}$ cells, which is consistent with a role for Doa4 in deubiquitinating MVB cargo proteins.

Interestingly, much more Ub-CPS was observed in *bro1*Δ cells compared with the level of Ub-CPS seen in *bro1*$^{\Delta CC}$ cells (Fig. 4 E), indicating that the deubiquitination of CPS is more severely compromised if the Bro1 protein is absent. Furthermore, the amount of Ub-CPS in *bro1*Δ mutants

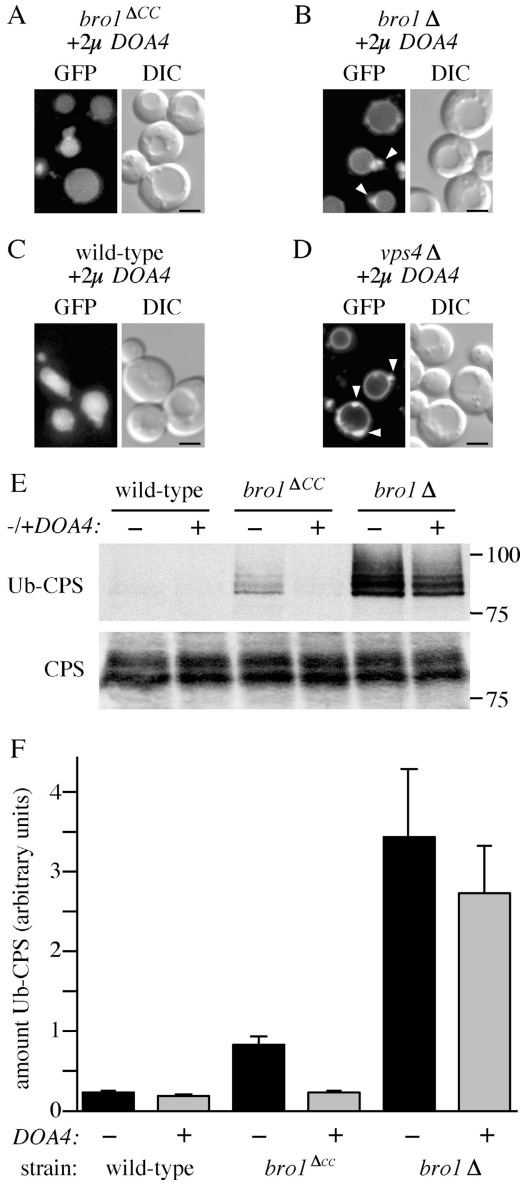

Figure 4. ***DOA4* overexpression in *bro1*$^{\Delta CC}$ mutant cells restores the sorting and deubiquitination of CPS.** (A–D) Fluorescence and DIC microscopy of GOY57 (A), KGY1 (B), BHY10 (C), and DBY42 (D) cells expressing the *GFP-CPS* fusion and transformed with 2 μ *DOA4*. Arrowheads indicate class compartments. Bars, 2.5 μm. (E) Immunoprecipitates of CPS were examined by Western blotting using anti-Ub or anti-CPS antibodies. Note that the lumenal domain of CPS is differentially glycosylated and is observed as a doublet. (F) Quantitation of the intensities of Ub-CPS versus CPS present in each lane in E. Bar graph depicts mean values ± SD from two independent experiments.

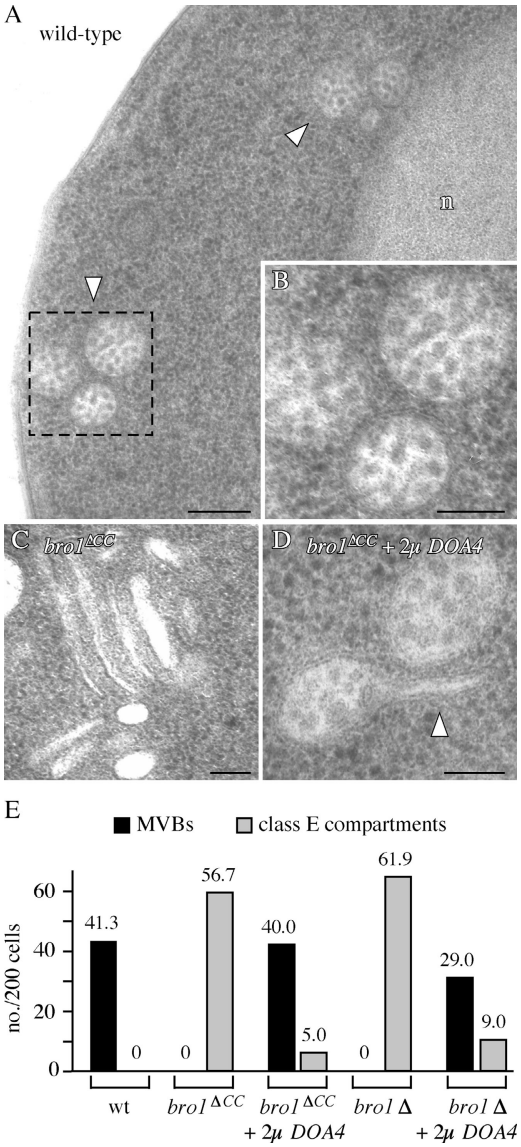

Figure 5. ***DOA4* overexpression restores MVB morphology in *bro1* mutant cells.** (A) EM showing MVBs in BHY10 cells. Arrowheads indicate MVBs. n, nucleus. Bar, 0.2 μm. (B) MVBs from the boxed area shown in A. Bar, 0.1 μm. (C) EM showing a typical class E compartment in GOY57 cells. Bar, 0.1 μm. (D) EM showing multivesicular structures in GOY57 cells transformed with 2 μ *DOA4*. The arrowhead indicates a tubule projecting from an MVB toward the cytoplasm; note that the membrane bilayer of the tubule is continuous with the bilayer surrounding the lumenal vesicles. Bar, 0.1 μm. (E) MVBs and class E compartments were counted in ~200 cells which had a diameter ≥ 2.5 μm. Each value is indicated above its respective bar in the graph and was expressed as the number per 200 cells. The multivesicular structures that had tubular projections (D, arrowhead) were counted as MVBs.

was much less significantly reduced upon overexpression of *DOA4*, in contrast with the complete restoration of CPS deubiquitination that occurred in *bro1*$^{\Delta CC}$ cells. This result is consistent with our observation that high-copy *DOA4* was much more effective at suppressing the GFP-CPS sorting defect in *bro1*$^{\Delta CC}$ cells (Fig. 4 A) versus *bro1*Δ cells (Fig. 4 B). Thus, excess amounts of Doa4 effectively alleviate the mutant phenotype caused by deletion of the Bro1 coiled-coil domain but cannot substitute for deletion of the entire Bro1 protein.

High-copy *DOA4* restores MVB morphology in *bro1* mutant cells

By fluorescence microscopy, it appeared that the overexpression of *DOA4* caused a reduction in the number of class E compartments in *bro1* mutant cells. Therefore, we used EM to examine the effect that high-copy *DOA4* has on endosomal ultrastructure. In wild-type cells, we readily observed MVBs, with each compartment consisting of a limiting

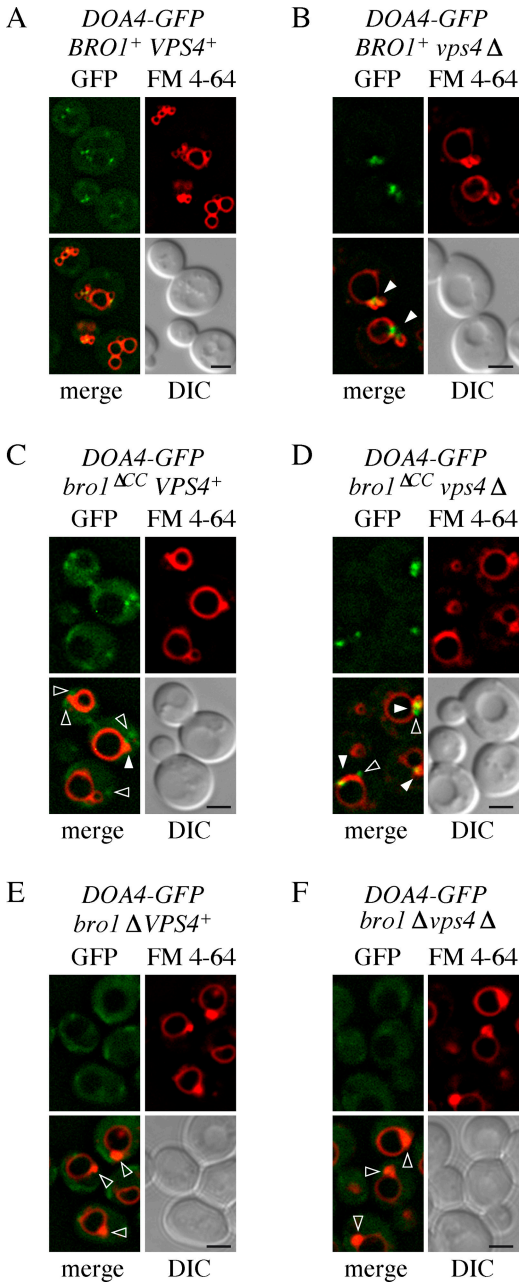

Figure 6. **Bro1 is required for the localization of Doa4 to endosomes.** Fluorescence and DIC microscopy of GOY74 (A), GOY75 (B), GOY88 (C), GOY93 (D), GOY82 (E), and GOY83 (F) cells stained with FM 4-64. Closed arrowheads indicate colocalization of GFP and FM 4-64 at class E compartments. In C and D, open arrowheads indicate GFP-positive structures not labeled by FM 4-64. In E and F, open arrowheads indicate FM 4-64–positive class E compartments at which Doa4-GFP is not localized. Bars, 2.5 μm.

membrane bilayer surrounding numerous vesicular profiles (Fig. 5, A and B). In contrast, MVBs were never evident in *bro1*$^{\Delta CC}$ or *bro1*Δ cells, which, instead, contained numerous class E compartments. An example of a class E compartment seen in *bro1*$^{\Delta CC}$ cells is shown in Fig. 5 C. Similar structures were also seen in *bro1*Δ cells (not depicted).

High-copy *DOA4* caused a striking change in endosomal morphology in *bro1*$^{\Delta CC}$ mutant cells. Rather than class E compartments, we observed numerous multivesicular structures, examples of which are shown in Fig. 5 D. These compartments consisted of a limiting membrane bilayer that encircled multiple vesicular profiles within the compartment lumen, which is similar to MVBs in wild-type cells (Fig. 5 B). Quantitative analysis indicated that *DOA4* overexpression in *bro1*$^{\Delta CC}$ cells caused a dramatic reduction in the number of class E compartments and resulted in almost as many MVBs as we had observed in wild-type cells (Fig. 5 E). The apparent reformation of MVBs and the concomitant disappearance of class E compartments upon *DOA4* overexpression occurred to a lesser extent in *bro1*Δ cells (Fig. 5 E), again indicating that high-copy *DOA4* is not as efficient at suppressing the phenotype caused by a total loss of Bro1 compared with its ability to suppress the phenotype caused by a deletion of only the Bro1 coiled-coil domain.

Interestingly, the overexpression of *DOA4* in *bro1* mutant cells occasionally resulted in multivesicular compartments having tubules projecting toward the cytoplasm that resemble the cisterna-like structures of class E compartments (Fig. 5 D, arrowhead). Although further studies are needed in order to establish the identity of these unusual structures, they may correspond to intermediate MVB/class E compartments.

The localization of Doa4 to endosomes requires Bro1

Doa4 had previously been shown to associate with endosomal compartments (Amerik et al., 2000). Indeed, when we integrated a *DOA4-GFP* gene fusion in place of the wild-type *DOA4* gene in cells that have normal Vps4 function (*VPS4*$^+$), we observed multiple fluorescent punctate structures in addition to diffuse cytoplasmic fluorescence (Fig. 6 A). This pattern of fluorescence resembles the intracellular localization of Bro1-GFP in *VPS4*$^+$ cells (Fig. 2 A). Also like Bro1-GFP, Doa4-GFP was concentrated at class E compartments in *vps4*Δ cells (Fig. 6 B). Doa4-GFP was also localized to class E compartments in *bro1*$^{\Delta CC}$ and *bro1*$^{\Delta CC}$ *vps4*Δ cells (Fig. 6, C and D, closed arrowheads), indicating that the Bro1 coiled-coil domain is not required for the association of Doa4 with late endosomes. Interestingly, Doa4-GFP was localized to additional punctate structures that were not labeled by FM 4-64 in *VPS4*$^+$ and *vps4*Δ cells expressing the mutant *bro1*$^{\Delta CC}$ allele in place of the wild-type *BRO1* gene (Fig. 6, C and D, open arrowheads), which is similar to the localization pattern of the mutant bro1$^{\Delta CC}$-GFP protein (Fig. 2, C and D).

A dramatic change in the localization of Doa4-GFP occurred in cells in which the *BRO1* gene had been deleted. Both in *bro1*Δ cells (Fig. 6 E) and *bro1*Δ *vps4*Δ double mutant cells (Fig. 6 F), Doa4-GFP failed to localize to class E compartments and was, instead, diffusely distributed. Some faintly fluorescent structures were evident at the periphery of these cells but are unlikely to be endosomes, as they were never stained when FM 4-64 was incubated continuously with cells (unpublished data), a procedure that results in staining of all compartments of the endocytic pathway (Vida and Emr, 1995). Western blot analysis confirmed that the expression of full-length Doa4-GFP in *bro1*Δ and *bro1*Δ *vps4*Δ double mutant cells was equivalent to its expression in wild-type and *vps4*Δ cells (Fig. S1, available at http://www.jcb.org/cgi/content/full/jcb.200403139/DC1), indicating that the loss of punctate localization of Doa4-GFP in the

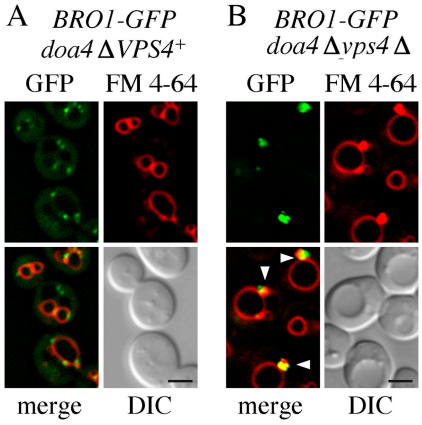

Figure 7. **Doa4 is not required for the localization of Bro1 to endosomes.** Fluorescence and DIC microscopy of GOY69 (A) and GOY70 (B) cells stained with FM 4-64. Arrowheads indicate class E compartments. Bars, 2.5 μm.

absence of Bro1 was not due to aberrant cleavage of the fusion protein. Furthermore, transformation of a plasmid encoding the wild-type *BRO1* gene into *bro1*Δ and *bro1*Δ *vps4*Δ cells restored the localization of Doa4-GFP to endosomal compartments (unpublished data). Thus, Bro1 is essential for the localization of Doa4 to endosomes.

To test whether the endosomal localization of Bro1 is likewise dependent on Doa4, we examined the localization of Bro1-GFP in cells in which the *DOA4* gene had been deleted. In *doa4*Δ *VPS4*$^+$ cells, we observed punctate fluorescent structures in addition to diffuse cytoplasmic fluorescence (Fig. 7 A), whereas in *doa4*Δ *vps4*Δ double mutant cells, the GFP fluorescence was concentrated at class E compartments (Fig. 7 B). This pattern of fluorescence was virtually identical to the intracellular localization of Bro1-GFP in *VPS4*$^+$ and *vps4*Δ cells (Fig. 2). Therefore, Doa4 is not required for the endosomal localization of Bro1.

Doa4 interacts with Bro1

Because Bro1 is required for the endosomal localization of Doa4, we investigated whether Doa4 physically interacts with Bro1 by immunoprecipitating the Doa4-GFP fusion protein from detergent-solubilized extracts of yeast cell lysates under native conditions. As shown in Fig. 8 A, Bro1-HA and bro1$^{\Delta CC}$-HA fusion proteins coimmunoprecipitated with Doa4-GFP from total extracts of *VPS4*$^+$ and *vps4*Δ cells. Control immunoprecipitations from lysates of strains not expressing *DOA4-GFP* confirmed that the isolation of Bro1-HA using anti-GFP antiserum required Doa4 (Fig. S2, available at http://www.jcb.org/cgi/content/full/jcb.200403139/DC1). Furthermore, the interaction between Bro1-HA and Doa4-GFP also occurred in anti-HA immunoprecipitations followed by anti-GFP Western blots (unpublished data).

We tested whether the interaction between Doa4 and Bro1 occurred on membranes and/or in the cytoplasm by centrifuging cell lysates before immunoprecipitation in order to generate a pellet fraction enriched in late endosomal membranes and a supernatant fraction containing soluble proteins (Odorizzi et al., 2003). As shown in Fig. 8 B, more

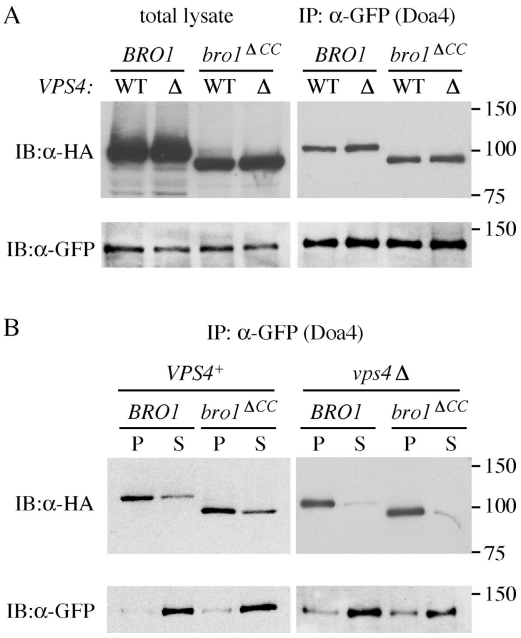

Figure 8. **Doa4 interacts with Bro1 and the mutant Bro1$^{\Delta CC}$ protein on membranes.** (A) Detergent extracts of total lysates from GOY107, GOY108, GOY106, and GOY105 cells were subjected to immunoprecipitation with rabbit anti-GFP polyclonal antiserum under native conditions and examined by Western blotting. (B) Cell lysates were separated into membrane pellet (P) and soluble (S) fractions and extracted with detergent before immunoprecipitation and Western blot analysis.

Bro1-HA and bro1$^{\Delta CC}$-HA coimmunoprecipitated with Doa4-GFP from the membrane fraction of *VPS4*$^+$ cells; however, these interactions were more significantly enriched in membrane extracts considering that the vast majority of Doa4-GFP in *VPS4*$^+$ cells was recovered from the soluble fraction (Fig. 8 B). In *vps4*Δ cells, the interaction between Doa4-GFP and both Bro1-HA and bro1$^{\Delta CC}$-HA occurred almost exclusively in the membrane fraction, again despite the fact that more Doa4-GFP was immunoprecipitated from the soluble fraction (Fig. 8 B). Altogether, these results indicate that Doa4 associates with Bro1 on membranes and that the coiled-coil domain is not required for this interaction to occur.

Endosomal localization of Doa4 in ESCRT-III mutant cells

A previous study had suggested that the association of Doa4 with endosomes was dependent on two other class E Vps proteins, Vps24 and Snf7 (Amerik et al., 2000). Both Vps24 and Snf7 are components of the ESCRT-III complex that oligomerizes on endosomal membranes (Babst et al., 2002a). We recently showed that the endosomal localization of Bro1 requires Snf7 but not Vps24, suggesting that Snf7 has a role in the recruitment or stabilization of Bro1 at endosomes (Odorizzi et al., 2003). Therefore, we examined the localization of Doa4-GFP in *vps4*Δ cells in which either *VPS24* or *SNF7* had been deleted. In contrast with the previous analysis of Doa4 localization (Amerik et al., 2000), we observed Doa4-GFP at class E compartments in *vps24*Δ *vps4*Δ double mutant cells (Fig. 9 A). However, Doa4-GFP was diffusely dis-

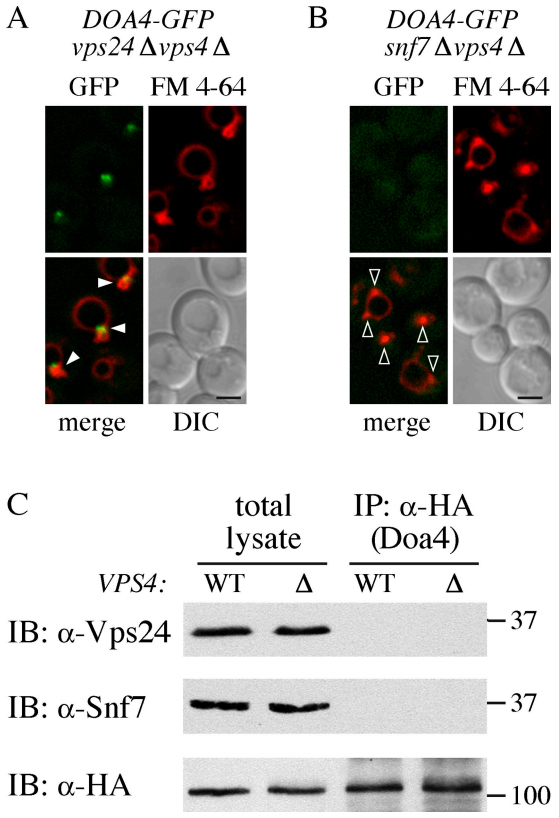

Figure 9. **Localization of Doa4-GFP in ESCRT-III mutants.** (A and B) Fluorescence and DIC microscopy of GOY113 (A) and GOY114 (B) cells stained with FM 4-64. Closed arrowheads indicate colocalization of Doa4-GFP and FM 4-64 at class E compartments. Open arrowheads indicate class E compartments at which Doa4-GFP is not localized. Bars, 2.5 μm. (C) Native immunoprecipitations from detergent extracts of total lysates of GOY115 and GOY116 cells.

tributed in *snf7*Δ *vps4*Δ double mutants (Fig. 9 B). This pattern in the localization of Doa4-GFP was identical to the localization of Bro1 that we had previously observed in these same mutant strains (Odorizzi et al., 2003). The inability of Doa4-GFP to localize to endosomal compartments in the absence of Snf7 may, therefore, be due to the requirement for Snf7 in the endosomal localization of Bro1 (Odorizzi et al., 2003). Indeed, as shown in Fig. 9 C, neither Vps24 nor Snf7 coimmunoprecipitated with Doa4 from *VPS4*$^{+}$ or *vps4*Δ cell extracts. Thus, the ESCRT-III complex does not appear to have a direct role in the recruitment of Doa4 to endosomes.

Discussion

Protein sorting in the MVB pathway requires Bro1, a cytoplasmic protein that associates with endosomal compartments (Odorizzi et al., 2003). Here, we show that *DOA4* overexpression suppresses the defects in MVB transport and restores the multivesicular morphology of endosomes in *bro1* mutant cells. These observations can be explained by our finding that Bro1 associates with Doa4 on endosomal membranes and that the recruitment of Doa4 to endosomes requires Bro1. Thus, our results indicate a key role for Bro1 in regulating the timing and location of Doa4 activity in the MVB pathway.

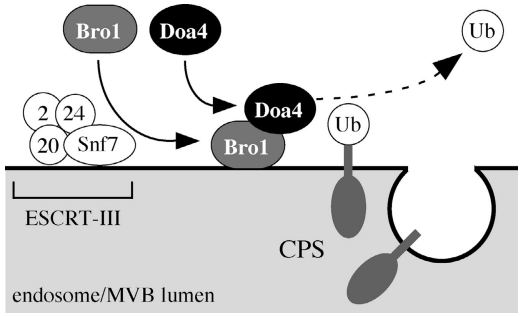

Figure 10. **Model for the recruitment of Doa4 to endosomes by Bro1.** Bro1 is required for the association of Doa4 with endosomes, where Doa4 catalyzes deubiquitination of MVB cargo proteins. The endosomal recruitment of Bro1, and consequently the recruitment of Doa4, is dependent on Snf7, which oligomerizes on endosomal membranes with the other ESCRT-III components (Vps2, Vps24, and Vps20). After their deubiquitination, MVB cargoes are sorted into lumenal vesicles. Not depicted is the dissociation of Bro1, Doa4, and ESCRT-III proteins from endosomes, which is catalyzed by the Vps4 ATPase.

Recruitment of Doa4 by Bro1

Both Doa4-GFP and Bro1-GFP were associated with endosomal compartments, but upon deletion of the *BRO1* gene, the localization of Doa4-GFP was shifted to the cytoplasm. In contrast, Bro1-GFP remained associated with endosomes regardless of whether the *DOA4* gene had been deleted. Native immunoprecipitation experiments revealed a physical interaction between Doa4 and Bro1, which could reflect direct binding of Doa4 by Bro1 or, alternatively, could be mediated by another component that binds both proteins. In either case, the association of Doa4 with Bro1 occurred predominantly in subcellular fractions containing late endosomal membranes, which is consistent with the ordered recruitment of Bro1 to endosomes followed by the recruitment of Doa4 (Fig. 10). Consistent with this model, the association of Doa4-GFP with endosomes required Snf7, a component of the ESCRT-III complex. We recently showed that Snf7 is essential for the endosomal localization of Bro1 (Odorizzi et al., 2003), and in mammalian cells, the orthologue of Bro1, Alix/Aip1, binds Chmp4b, which is an orthologue of Snf7 (Katoh et al., 2003; Martin-Serrano et al., 2003; Strack et al., 2003; von Schwedler et al., 2003; Peck et al., 2004). Thus, it is likely that Snf7 has an indirect role in the endosomal localization of Doa4 by functioning to recruit Bro1 to endosomes or to stabilize the association of Bro1 with endosomal membranes. Indeed, we were unable to detect a physical interaction between Doa4 and either Snf7 or Vps24, another component of the ESCRT-III complex. Furthermore, high-copy *DOA4* could not suppress the defects in either CPY or CPS sorting caused by the loss of any ESCRT-III component.

It is unlikely that Snf7 recruits Bro1 to endosomes by interacting with the Bro1 coiled-coil domain, as this region of Bro1 was not required for its association with endosomal membranes. Furthermore, despite the fact that we identified *DOA4* in a screen for high-copy suppressors of the *bro1*$^{\Delta CC}$ mutant phenotype, the Bro1 coiled-coil domain is not necessary for Bro1 to interact with Doa4. Nevertheless, the coiled-coil domain is important for Bro1 function, as the

transport of GFP-CPS was blocked in *bro1*$^{\Delta CC}$ mutant cells as effectively as it was in *bro1*Δ cells. Therefore, the recruitment of Doa4 to endosomes is only one aspect of the function of Bro1 in the MVB pathway. The role of the Bro1 coiled-coil domain is not yet clear. Thus far, we have been unable to identify another protein that interacts with this region of Bro1, and we have been unable to detect homo-oligomerization of Bro1 that could be mediated by the coiled-coil domain (unpublished data).

Suppression by high-copy *DOA4*

The restoration of multivesicular structures upon the overexpression of *DOA4* coincided with the disappearance of class E compartments, which presumably enables the CPY receptor, Vps10, to recycle to the Golgi where it binds newly synthesized CPY-Inv in order to transport this soluble cargo protein to the endosome (Cereghino et al., 1995; Cooper and Stevens, 1996). Accordingly, we have observed that a Vps10-GFP fusion protein was not concentrated at class E compartments in *bro1* mutant cells overexpressing *DOA4* but was, instead, localized to multiple punctate structures (unpublished data), which is similar to its localization in wild-type cells (Burda et al., 2002; Odorizzi et al., 2003).

Interestingly, although high-copy *DOA4* restored the multivesicular morphology of late endosomes and suppressed CPY-Inv secretion by both *bro1*$^{\Delta CC}$ and *bro1*Δ cells, the transport of GFP-CPS via the MVB pathway was efficiently restored by *DOA4* overexpression only in *bro1*$^{\Delta CC}$ and not *bro1*Δ cells. Furthermore, the overexpression of *DOA4* in *bro1*Δ cells did not significantly enhance the deubiquitination of CPS, whereas the minor amount of Ub-CPS seen in the *bro1*$^{\Delta CC}$ strain was completely eliminated by *DOA4* overexpression. These observations are consistent with the ability of Doa4 to be recruited to endosomes in cells expressing the mutant bro1$^{\Delta CC}$ protein but not in cells in which Bro1 is completely absent. Moreover, these findings suggest that restoring MVB morphology alone by *DOA4* overexpression is not sufficient for a complete restoration of the MVB pathway. The overexpression of *DOA4* in *bro1*Δ cells may result in excess amounts of Doa4 that could deubiquitinate proteins which regulate the formation of MVB vesicles, but the sorting of cargoes into MVB vesicles per se may be critically dependent on the coordination of Doa4 on endosomal membranes by Bro1 as well as other aspects of Bro1 function in the MVB pathway.

Deubiquitination in the MVB pathway

Ubiquitination is tightly controlled by Ub-conjugation enzymes and is counterbalanced by deubiquitination. Both poly- and monoubiquitinated proteins undergo deubiquitination, but few Ub thiolesterases have been assigned to specific substrates (Wing, 2003). There are 16 UBPs in *S. cerevisiae*, suggesting that many of these enzymes have highly specific and regulated functions. However, Doa4 probably has a wide variety of substrates. In addition to its role in the removal of monoubiquitin from MVB cargo proteins, Doa4 is likely to function in the removal of polyubiquitin from proteasomal substrates, as Doa4 copurifies with proteasomes that have been isolated from yeast cell extracts (Papa et al., 1999).

Consistent with a role for Bro1 in coordinating Doa4 function are the previous observations that Bro1 is required for the deubiquitination of CPS (Odorizzi et al., 2003) as well as Gap1, an amino acid permease at the plasma membrane that is down-regulated by endocytosis and sorted via the MVB pathway (Nikko et al., 2003). Interestingly, in *bro1* mutant cells, Gap1 is recycled to the plasma membrane but, unlike CPS, does not accumulate in its ubiquitinated form. However, ubiquitinated Gap1 is readily detected in *bro1* mutant cells if recycling is blocked, suggesting that in the absence of Bro1, the deubiquitination of Gap1 (and possibly other endocytic cargoes) occurs elsewhere within the cell and may be catalyzed by one of the 15 other UBPs in yeast (Nikko et al., 2003).

The suppressor activity of high-copy *DOA4* was abolished if the putative active-site cysteine residue was altered to serine, indicating that suppression most likely occurred through substrate deubiquitination. However, the deubiquitination of cargoes is not essential for MVB sorting because chimeric cargo proteins that are expressed as translational fusions to Ub cannot be deubiquitinated yet are transported efficiently via the MVB pathway (Reggiori and Pelham, 2001; Urbanowski and Piper, 2001; Bilodeau et al., 2003). Nevertheless, Doa4 is required for the MVB pathway, as the sorting of MVB cargo proteins is blocked in *doa4* mutant cells (Losko et al., 2001; Reggiori and Pelham, 2001). In addition to MVB cargoes, Doa4 could deubiquitinate a component of the MVB sorting machinery in order to regulate its activity. It is not known whether class E Vps proteins in yeast are regulated by ubiquitination. In mammalian cells, however, several cytoplasmic proteins that control receptor down-regulation are monoubiquitinated, including Hrs, which is the orthologue of the yeast class E Vps protein, Vps27 (Polo et al., 2002). CIN85 and endophilin are also monoubiquitinated cytoplasmic components in mammalian cells that associate with endosomes (Haglund et al., 2002; Angers et al., 2004), and both proteins interact with Alix/Aip1 (Vito et al., 1996; Chatellard-Causse et al., 2002). Like Bro1 in yeast, Alix/Aip1 could recruit a UBP that deubiquitinates CIN85 and endophilin in order to regulate their function and/or localization.

Our results suggest a model in which Bro1 recruits Doa4 to endosomal membranes, thereby controlling the timing and location of Doa4 activity in the MVB pathway (Fig. 10). The association of Bro1 itself with endosomes occurs after the assembly of the ESCRT-III complex on endosomes (Odorizzi et al., 2003). Similarly, the deubiquitination of MVB cargo proteins occurs downstream of the functions of the ESCRT-I, -II, and -III complexes (Nikko et al., 2003) but before enclosure of cargoes within MVB vesicles (Hicke and Dunn, 2003). Thus, the Bro1-dependent coordination of Doa4 on endosomal membranes and the subsequent deubiquitination of cargo proteins (and possibly MVB sorting components) is likely to be one of the last steps in the MVB pathway, ensuring that cargo proteins are concentrated at regions of the endosomal membrane where invagination occurs. In mammalian cells, the assembly/budding of HIV-1 depends on ubiquitination of the viral Gag protein (for review see Pornillos et al.,

2002), but a role for deubiquitination in this process has not been described. However, recent studies indicate that Alix/Aip1 interacts with both the ESCRT-I and -III complexes and is involved in viral escape from host cells (Strack et al., 2003; von Schwedler et al., 2003). Future studies may determine whether Alix/Aip1 has a role analogous to Bro1 and functions in the recruitment of a specific UBP to the site of viral budding.

Materials and methods

Yeast strains and plasmid constructions

Standard protocols were used for culturing *S. cerevisiae*, cellular transformations, and spheroplast preparations (Guthrie and Fink, 2002). See Table II for the genotypes of yeast strains used in this work. Gene deletions were constructed by homologous recombination using site-specific deletion cassettes (Guthrie and Fink, 2002).

To construct the *bro1*$^{\Delta CC}$ allele, the SpeI–SalI fragment containing the *BRO1* gene in plasmid pGO187 (Odorizzi et al., 2003) was subcloned into SpeI–SalI-digested pRS413, resulting in plasmid pGO263, which was digested with EcoRV and recircularized using T4 DNA ligase. The resulting plasmid (pGO265) contained the mutant *bro1*$^{\Delta CC}$ allele consisting of codon 540 adjoined to codon 586. The SpeI–SalI fragment in pGO265 was subcloned into SpeI–SalI-digested pRS416, pRS426, and pRS306, resulting in pGO273, pGO272, and pGO287, respectively. The *bro1*$^{\Delta CC}$ allele was integrated into the genome in place of the wild-type *BRO1* gene using pGO287 by homologous recombination (Guthrie and Fink, 2002). The *doa4*$^{C/S}$ allele was constructed by PCR and subcloned into pRS202, resulting in pGO309.

Microscopy

GFP and FM 4-64 fluorescence and differential interference contrast (DIC) microscopy was performed using a DMRXA microscope (Leica) equipped with a Cooke Sensicam digital camera (Applied Scientific Instruments). Images were deconvolved using Slidebook® software (Intelligent Imaging Innovations) and processed using Adobe Photoshop 7.0® software (Adobe Systems Inc.). Cells were stained with FM 4-64 using a pulse-chase proce-

Table II. **Yeast strains used in this work**

Strain	Genotype	Reference
SEY6210	*MATα leu2-3,112 ura3-52 his3Δ200 trp1-Δ901 lys2-Δ801 suc2-Δ9*	Robinson et al., 1988
BHY10	SEY6210; *leu2-3,112*::pBHY11	Horazdovsky et al., 1994
GOY57	BHY10; *bro1*$^{\Delta CC}$	This work
KGY1	BHY10; *bro1Δ::HIS3*	This work
DMY1	SEY6210; *BRO1-GFP::HIS3*	This work
DMY2	SEY6210; *BRO1-GFP::HIS3 vps4Δ::TRP1*	This work
DBY15	BHY10; *bro1*$^{\Delta CC}$*-GFP::HIS3*	This work
DBY18	BHY10; *bro1*$^{\Delta CC}$*-GFP::HIS3 vps4Δ::TRP1*	This work
GOY23	SEY6210; *pep4Δ::LEU2 prb1Δ::LEU2*	This work
GOY71	GOY23; *bro1*$^{\Delta CC}$	This work
DBY43	GOY23; *bro1Δ::HIS3*	This work
GOY74	SEY6210; *DOA4-GFP::HIS3*	This work
GOY75	SEY6210; *DOA4-GFP::HIS3 vps4Δ::TRP1*	This work
GOY88	SEY6210; *DOA4-GFP::HIS3 bro1*$^{\Delta CC}$	This work
GOY93	SEY6210; *DOA4-GFP::HIS3 bro1*$^{\Delta CC}$ *vps4Δ::TRP1*	This work
GOY82	SEY6210; *DOA4-GFP::HIS3 bro1Δ::KAN*	This work
GOY83	SEY6210; *DOA4-GFP::HIS3 bro1Δ::KAN vps4Δ::TRP1*	This work
GOY69	SEY6210; *BRO1-GFP::HIS3 doa4Δ::KAN*	This work
GOY70	SEY6210; *BRO1-GFP::HIS3 doa4Δ::KAN vps4Δ::TRP1*	This work
GOY113	SEY6210; *DOA4-GFP::KAN vps4Δ::TRP1 vps24Δ::HIS3*	This work
GOY114	SEY6210; *DOA4-GFP::KAN vps4Δ::TRP1 snf7Δ::HIS3*	This work
GOY107	GOY23; *DOA4-GFP::KAN BRO1-HA::HIS3*	This work
GOY108	GOY23; *DOA4-GFP::KAN BRO1-HA::HIS3 vps4Δ::TRP1*	This work
GOY106	GOY23; *DOA4-GFP::KAN bro1*$^{\Delta CC}$*-HA::HIS3*	This work
GOY105	GOY23; *DOA4-GFP::KAN bro1*$^{\Delta CC}$*-HA::HIS3 vps4Δ::TRP1*	This work
DBY42	BHY10; *vps4Δ::TRP1*	This work
NLY25	BHY10; *bro1Δ::HIS3 vps4Δ::TRP1*	This work
DBY24	BHY10; *bro1*$^{\Delta CC}$ *vps4Δ::TRP1*	This work
GOY86	BHY10; *vps23Δ::HIS3*	This work
NLY10	BHY10; *vps28Δ::HIS3*	This work
NLY8	BHY10; *vps37Δ::HIS3*	This work
GOY85	BHY10; *vps22Δ::HIS3*	This work
GOY78	BHY10; *vps25Δ::HIS3*	This work
CRY2	BHY10; *vps36Δ::HIS3*	This work
GOY79	BHY10; *vps2Δ::HIS3*	This work
CRY1	BHY10; *vps24Δ::HIS3*	This work
GOY80	BHY10; *vps20Δ::HIS3*	This work
GOY81	BHY10; *snf7Δ::HIS3*	This work
GOY87	BHY10; *vps27Δ::HIS3*	This work
GOY91	BHY10; *nhx1Δ::HIS3*	This work
GOY90	BHY10; *vps60Δ::HIS3*	This work

dure at 30°C as described previously (Odorizzi et al., 2003). To observe the localization of GFP-CPS, cells were transformed with pGO47, which contains the *GFP-CPS* fusion (Odorizzi et al., 1998). For EM, cells growing logarithmically at 30°C were high pressure frozen, freeze substituted, sectioned, and stained as described in Giddings (2003). Thin sections were viewed with a CM10 electron microscope (Philips) and images were captured on film. For quantitation, the number of multivesicular structures and class E compartments were counted in ~200 randomly chosen cells measuring at least 2.5 μm in diameter.

Genetic screen for high-copy suppressors of *bro1*$^{\Delta CC}$

GOY57 cells were transformed with a high-copy library of yeast genomic DNA in plasmid pRS202 (*2 μ URA3*). Transformants were screened for secreted invertase activity using the agar overlay assay described in Darsow et al. (2000). Library plasmids that reliably displayed suppression were recovered and transformed into naïve GOY57 cells to confirm that the suppression was plasmid linked. One plasmid (designated pGO289) identified as a suppressor of the *bro1*$^{\Delta CC}$ phenotype contained a fragment of chromosome IV. To confirm that the *DOA4* gene in this region of the chromosome was responsible for suppression, the *DOA4* coding sequence was deleted from pGO289 (resulting in pGO302), and the *DOA4* gene alone was subcloned into pRS202 (resulting in pMD10). pMD10 was found to suppress CPY-Inv as effectively as pGO289, whereas pGO302 was incapable of suppression. Quantitative measurements of the amount of secreted invertase activity were performed in triplicate in at least three independent experiments using the liquid assay described in Darsow et al. (2000).

Immunoprecipitations and Western blotting

Detection of Ub-CPS was performed as described in Katzmann et al. (2001). In the strains that were examined, the *PEP4* and *PRB1* genes, which encode vacuolar proteases, had been deleted in order to reduce the nonspecific cleavage of Ub from CPS after cell lysis. The amount of Ub-CPS versus CPS in each lane was quantitated using Adobe Photoshop 7.0®. For native immunoprecipitations, 20 A_{600} equivalents of yeast cells were converted to spheroplasts, osmotically lysed in 2-ml ice-cold lysis buffer (200 mM sorbitol, 50 mM potassium acetate, 20 mM Hepes, pH 7.2, 2 mM EDTA, supplemented with a protease inhibitor cocktail; Roche), and homogenized on ice. Triton X-100 was added to a final concentration of 0.5%, the lysates were rotated at 4°C for 10 min, and then centrifuged at 16,000 *g* in order to pellet the detergent-insoluble material. Five A_{600} equivalents of the detergent-soluble extract were precipitated by the addition of 10% (vol/vol) TCA, resulting in a sample representing the total lysate. Rabbit anti-GFP polyclonal antiserum (provided by C. Zuker, University of California, San Diego, La Jolla, CA) plus protein A-Sepharose beads or mouse anti-HA mAbs plus γ-bind Sepharose beads (Amersham Biosciences) were added to 10 A_{600} equivalents of the remaining detergent-soluble extract, which was rotated at 4°C for 2 h. Immune complexes were recovered by centrifugation at 4°C, washed twice with ice-cold lysis buffer plus 0.5% Triton X-100, and twice with ice-cold lysis buffer. Bound antigen was eluted by boiling the beads in SDS-PAGE sample buffer. Four A_{600} equivalents of immunoprecipitates and 0.5 A_{600} equivalents of total lysate were resolved by SDS-PAGE, transferred to nitrocellulose, and examined by Western blotting using anti-GFP mAbs (Zymed Laboratories), anti-HA mAbs (Roche), or polyclonal antisera against Snf7 and Vps24 (Babst et al., 1998).

Online supplemental material

Fig. S1 shows that there is not a significant difference in the expression levels of full-length Doa4-GFP in the strains shown in Fig. 6. Fig. S2 shows the results from a negative control for Fig. 8 in which Bro1-HA is not immunoprecipitated under native conditions by anti-GFP antiserum in the absence of Doa4-GFP expression. Online supplemental material is available at http://www.jcb.org/cgi/content/full/jcb.200403139/DC1.

We thank Jeff Kimes and Tom Giddings for EM, Monica Darland for construction of plasmids, Doug Burch, David Mellman, Caleb Richter, and Kelly Geiger for construction of yeast strains (University of Colorado), and Charles Zuker for providing rabbit anti-GFP polyclonal antiserum.

G. Odorizzi is supported by an American Cancer Society grant (RSG-02-147-01) and a National Institutes of Health grant (GM065505).

Submitted: 26 March 2004
Accepted: 6 July 2004

References

Amerik, A.Y., J. Nowak, S. Swaminathan, and M. Hochstrasser. 2000. The Doa4 deubiquitinating enzyme is functionally linked to the vacuolar protein-sorting and endocytic pathways. *Mol. Biol. Cell.* 11:3365–3380.

Angers, A., A.R. Ramjaun, and P.S. McPherson. 2004. The HECT domain ligase Itch ubiquitinates endophilin and localizes to the trans-Golgi network and endosomal system. *J. Biol. Chem.* 279:11471–11479.

Babst, M., B. Wendland, E.J. Estepa, and S.D. Emr. 1998. The Vps4p AAA ATPase regulates membrane association of a Vps protein complex required for normal endosome function. *EMBO J.* 17:2982–2993.

Babst, M., D.J. Katzmann, E.J. Estepa-Sabal, T. Meerloo, and S.D. Emr. 2002a. Escrt-III: an endosome-associated heterooligomeric protein complex required for mvb sorting. *Dev. Cell.* 3:271–282.

Babst, M., D.J. Katzmann, W.B. Snyder, B. Wendland, and S.D. Emr. 2002b. Endosome-associated complex, ESCRT-II, recruits transport machinery for protein sorting at the multivesicular body. *Dev. Cell.* 3:283–289.

Bilodeau, P.S., S.C. Winistorfer, W.R. Kearney, A.D. Robertson, and R.C. Piper. 2003. Vps27-Hse1 and ESCRT-I complexes cooperate to increase efficiency of sorting ubiquitinated proteins at the endosome. *J. Cell Biol.* 163:237–243.

Burda, P., S.M. Padilla, S. Sarkar, and S.D. Emr. 2002. Retromer function in endosome-to-Golgi retrograde transport is regulated by the yeast Vps34 PtdIns 3-kinase. *J. Cell Sci.* 115:3889–3900.

Cereghino, J.L., E.G. Marcusson, and S.D. Emr. 1995. The cytoplasmic tail domain of the vacuolar protein sorting receptor Vps10p and a subset of VPS gene products regulate receptor stability, function, and localization. *Mol. Biol. Cell.* 6:1089–1102.

Chatellard-Causse, C., B. Blot, N. Cristina, S. Torch, M. Missotten, and R. Sadoul. 2002. Alix (ALG-2-interacting protein X), a protein involved in apoptosis, binds to endophilins and induces cytoplasmic vacuolization. *J. Biol. Chem.* 277:29108–29115.

Cooper, A.A., and T.H. Stevens. 1996. Vps10p cycles between the late-Golgi and prevacuolar compartments in its function as the sorting receptor for multiple yeast vacuolar hydrolases. *J. Cell Biol.* 133:529–541.

Darsow, T., G. Odorizzi, and S.D. Emr. 2000. Invertase fusion proteins for analysis of protein trafficking in yeast. *Methods Enzymol.* 327:95–106.

Dupre, S., and R. Haguenauer-Tsapis. 2001. Deubiquitination step in the endocytic pathway of yeast plasma membrane proteins: crucial role of Doa4p ubiquitin isopeptidase. *Mol. Cell. Biol.* 21:4482–4494.

Giddings, T.H. 2003. Freeze-substitution protocols for improved visualization of membranes in high-pressure frozen samples. *J. Microsc.* 212:53–61.

Guthrie, C., and G.R. Fink. 2002. Guide to yeast genetics and molecular biology. Vol. 350. Academic Press, San Diego. Part B. 623 pp.

Haglund, K., N. Shimokawa, I. Szymkiewicz, and I. Dikic. 2002. Cbl-directed monoubiquitination of CIN85 is involved in regulation of ligand-induced degradation of EGF receptors. *Proc. Natl. Acad. Sci. USA.* 99:12191–12196.

Hicke, L., and R. Dunn. 2003. Regulation of membrane protein transport by ubiquitin and ubiquitin-binding proteins. *Annu. Rev. Cell Dev. Biol.* 19:141–172.

Horazdovsky, B.F., G.R. Busch, and S.D. Emr. 1994. VPS21 encodes a rab5-like GTP binding protein that is required for the sorting of yeast vacuolar proteins. *EMBO J.* 13:1297–1309.

Hu, M., P. Li, M. Li, W. Li, T. Yao, J.W. Wu, W. Gu, R.E. Cohen, and Y. Shi. 2002. Crystal structure of a UBP-family deubiquitinating enzyme in isolation and in complex with ubiquitin aldehyde. *Cell.* 111:1041–1054.

Katoh, K., H. Shibata, H. Suzuki, A. Nara, K. Ishidoh, E. Kominami, T. Yoshimori, and M. Maki. 2003. The ALG-2-interacting protein Alix associates with CHMP4b, a human homologue of yeast Snf7 that is involved in multivesicular body sorting. *J. Biol. Chem.* 278:39104–39113.

Katzmann, D.J., M. Babst, and S.D. Emr. 2001. Ubiquitin-dependent sorting into the multivesicular body pathway requires the function of a conserved endosomal protein sorting complex, ESCRT-I. *Cell.* 106:145–155.

Katzmann, D.J., C.J. Stefan, M. Babst, and S.D. Emr. 2003. Vps27 recruits ESCRT machinery to endosomes during MVB sorting. *J. Cell Biol.* 162:413–423.

Losko, S., F. Kopp, A. Kranz, and R. Kolling. 2001. Uptake of the ATP-binding cassette (ABC) transporter Ste6 into the yeast vacuole is blocked in the doa4 mutant. *Mol. Biol. Cell.* 12:1047–1059.

Martin-Serrano, J., A. Yarovoy, D. Perez-Caballero, and P.D. Bieniasz. 2003. Divergent retroviral late-budding domains recruit vacuolar protein sorting factors by using alternative adaptor proteins. *Proc. Natl. Acad. Sci. USA.* 100: 12414–12419.

Matsuo, H., J. Chevallier, N. Mayran, I. Le Blanc, C. Ferguson, J. Faure, N.S. Blanc, S. Matile, J. Dubochet, R. Sadoul, et al. 2004. Role of LBPA and Alix in multivesicular liposome formation and endosome organization. *Science.*

303:531–534.

Nikko, E., A.M. Marini, and B. Andre. 2003. Permease recycling and ubiquitination status reveal a particular role for Bro1 in the multivesicular body pathway. *J. Biol. Chem.* 278:50732–50743.

Odorizzi, G., M. Babst, and S.D. Emr. 1998. Fab1p PtdIns(3)P 5-kinase function essential for protein sorting in the multivesicular body. *Cell.* 95:847–858.

Odorizzi, G., D.J. Katzmann, M. Babst, A. Audhya, and S.D. Emr. 2003. Bro1 is an endosome-associated protein that functions in the MVB pathway in *Saccharomyces cerevisiae*. *J. Cell Sci.* 116:1893–1903.

Papa, F.R., A.Y. Amerik, and M. Hochstrasser. 1999. Interaction of the Doa4 deubiquitinating enzyme with the yeast 26S proteasome. *Mol. Biol. Cell.* 10:741–756.

Peck, J.W., E.T. Bowden, and P.D. Burbelo. 2004. Structure and function of human Vps20 and Snf7 proteins. *Biochem. J.* 377:693–700.

Polo, S., S. Sigismund, M. Faretta, M. Guidi, M.R. Capua, G. Bossi, H. Chen, P. De Camilli, and P.P. Di Fiore. 2002. A single motif responsible for ubiquitin recognition and monoubiquitination in endocytic proteins. *Nature.* 416:451–455.

Pornillos, O., S.L. Alam, R.L. Rich, D.G. Myszka, D.R. Davis, and W.I. Sundquist. 2002. Structure and functional interactions of the Tsg101 UEV domain. *EMBO J.* 21:2397–2406.

Reggiori, F., and H.R. Pelham. 2001. Sorting of proteins into multivesicular bodies: ubiquitin-dependent and -independent targeting. *EMBO J.* 20:5176–5186.

Robinson, J.S., D.J. Klionsky, L.M. Banta, and S.D. Emr. 1988. Protein sorting in *Saccharomyces cerevisiae*: isolation of mutants defective in the delivery and processing of multiple vacuolar hydrolases. *Mol. Cell. Biol.* 8:4936–4948.

Strack, B., A. Calistri, S. Craig, E. Popova, and H.G. Gottlinger. 2003. AIP1/ALIX is a binding partner for HIV-1 p6 and EIAV p9 functioning in virus budding. *Cell.* 114:689–699.

Urbanowski, J.L., and R.C. Piper. 2001. Ubiquitin sorts proteins into the intralumenal degradative compartment of the late-endosome/vacuole. *Traffic.* 2:622–630.

Vida, T.A., and S.D. Emr. 1995. A new vital stain for visualizing vacuolar membrane dynamics and endocytosis in yeast. *J. Cell Biol.* 128:779–792.

Vito, P., E. Lacana, and L. D'Adamio. 1996. Interfering with apoptosis: Ca^{2+}-binding protein ALG-2 and Alzheimer's disease gene ALG-3. *Science.* 271: 521–525.

von Schwedler, U.K., M. Stuchell, B. Muller, D.M. Ward, H.Y. Chung, E. Morita, H.E. Wang, T. Davis, G.P. He, D.M. Cimbora, et al. 2003. The protein network of HIV budding. *Cell.* 114:701–713.

Weissman, A.M. 2001. Themes and variations on ubiquitylation. *Nat. Rev. Mol. Cell Biol.* 2:169–178.

Wing, S.S. 2003. Deubiquitinating enzymes-the importance of driving in reverse along the ubiquitin-proteasome pathway. *Int. J. Bioch. Cell Biol.* 35:590–605.